Published in final edited form as:
Nat Immunol. 2010 June ; 11(6): 495–502. doi:10.1038/ni.1878.

Synaptotagmin-mediated vesicle fusion regulates cell migration

Richard A Colvin[1,8], **Terry K Means**[1], **Thomas J Diefenbach**[2], **Luis F Moita**[1,3], **Robert P Friday**[1], **Sanja Sever**[4], **Gabriele S V Campanella**[1], **Tabitha Abrazinski**[1], **Lindsay A Manice**[1], **Catarina Moita**[1,3], **Norma W Andrews**[5], **Dianqing Wu**[6], **Nir Hacohen**[1,7], and **Andrew D Luster**[1]

[1] Center for Immunology and Inflammatory Diseases, Division of Rheumatology, Allergy, and Immunology, Massachusetts General Hospital (MGH) and Harvard Medical School, Boston, Massachusetts, USA

[2] Ragon Institute of MGH, Massachusetts Institute of Technology (MIT) and Harvard, Boston, Massachusetts, USA

[3] Cell Biology of the Immune System Unit, Instituto de Medicina Molecular, Faculdade de Medicina, Universidade de Lisboa, Lisboa, Portugal

[4] Division of Nephrology, Massachusetts General Hospital, Boston, Massachusetts, USA

[5] Department of Cell Biology and Molecular Genetics, University of Maryland, College Park, Maryland, USA

[6] Yale University School of Medicine, Yale University, New Haven, Connecticut, USA

[7] Broad Institute, Cambridge, Massachusetts, USA

Abstract

Chemokines and other chemoattractants direct leukocyte migration and are essential for the development and delivery of immune and inflammatory responses. To probe the molecular mechanisms that underlie chemoattractant-guided migration, we did an RNA-mediated interference screen that identified several members of the synaptotagmin family of calcium-sensing vesicle-fusion proteins as mediators of cell migration: SYT7 and SYTL5 were positive regulators of chemotaxis, whereas SYT2 was a negative regulator of chemotaxis. SYT7-deficient leukocytes showed less migration *in vitro* and in a gout model *in vivo*. Chemoattractant-induced calcium-dependent lysosomal fusion was impaired in SYT7-deficient neutrophils. In a chemokine gradient, SYT7-deficient lymphocytes accumulated lysosomes in their uropods and had impaired uropod release. Our data identify a molecular pathway required for chemotaxis that links chemoattractant-induced calcium flux to exocytosis and uropod release.

Correspondence should be addressed to A.D.L. (aluster@mgh.harvard.edu).
[8]Present address: Novartis Institute for Biomedical Research, Cambridge, Massachusetts, USA.

Accession codes. UCSD-Nature Signaling Gateway (http://www.signaling-gateway.org): A000636, A002560, A002565 and A001978.

Note: Supplementary information is available on the Nature Immunology website.

AUTHOR CONTRIBUTIONS

R.A.C. designed the experiments, did the screening, collected and analyzed data and wrote the manuscript; T.K.M. did air-pouch experiments, macrophage stimulation and GTPase assays and helped edit the manuscript; T.J.D. did confocal microscopy and analyzed lymphocytes; L.F.M. and C.M. helped with initial screens; R.P.F. assisted with air-pouch experiments; S.S. did confocal microscopy of podocytes; G.S.V.C. helped with experiments; T.A. and L.A.M. collected data; N.W.A. provided mouse strains; D.W. assisted with video migration assays of neutrophils; N.H. helped design experiments, analyzed data and helped edit the manuscript; A.D.L. helped design experiments, analyzed data and edited the manuscript; and all authors discussed results and commented on the manuscript.

COMPETING FINANCIAL INTERESTS

The authors declare no competing financial interests.

Chemoattractant-directed cell migration is critical for the generation and delivery of immune and inflammatory responses[1]. Defining the molecular mechanisms that control directed cell movement is therefore essential for understanding the function of cells of the immune response, the host response to infection and tumors, and immune-mediated auto-immune and inflammatory diseases. Chemokines and other classical chemoattractants, such as formyl-Met-Leu-Phe (fMLP), C5a and leukotriene B_4, induce directed cell migration through the activation of seven-transmembrane-spanning G protein–coupled receptors[2]. Chemoattractant receptors form a related subfamily of ~50 G protein–coupled receptors that all couple to the pertussis toxin–sensitive cAMP-inhibitory heterotrimeric guanine nucleotide–binding protein G_i.

Chemokine receptors and other chemoattractant receptors are found on all leukocyte lineages. Activation of chemoattractant receptors transforms a chemical signal in the form of a gradient into a biophysical program that results in leukocyte shape change and directed cell movement[3]. A leading edge called the lamellopodia and a trailing edge called the uropod characterize the polarized migrating leukocyte that develops after activation of chemoattractant receptors. These complex changes involve cycles of membrane protrusions and contractions, polymerization and depolymerization of F-actin, and adhesion and de-adhesion. These processes are coordinated through the activation of multiple signaling pathways that are only partially understood[4,5].

After chemokines and chemoattractants bind to the extracellular domains of their cognate G protein–coupled receptor, the Gα and Gβγ subunits of G_i are liberated. The membrane-bound Gβγ subunits are thought to directly activate downstream signaling pathways, such as the β2 and β3 isoforms of phospholipase C (PLC)[6]. PLC then hydrolyzes phosphatidylinositol-(4,5)-bisphosphate to produce inositol-1,4,5-triphosphate ($Ins(1,4,5)P_3$) and diacyglycerol. $Ins(1,4,5)P_3$ induces the mobilization of intracellular calcium stores, which in turn has effects on calmodulin and myosin light-chain kinase[7,8]. An increase in intracellular free calcium is a hallmark of chemoattractant stimulation and has been linked to directional sensing, cytoskeleton redistribution, traction force regeneration and the relocation of focal adhesions[3,4,9,10].

The Gβγ subunits also activate phosphatidylinositol-3-OH kinase, which leads to changes in intracellular phosphatidylinositol-3,4,5-triphosphate[11,12]. Studies have indicated that phosphatidylinositol- (3,4,5)-triphosphate is an important mediator in the sensing of chemoattractant gradient, facilitating the recruitment of pleckstin homology domain–containing proteins to the cell membrane[13]. The Rho family of small GTPases, which includes Rac1, Cdc42 and RhoA, as well as their exchange factors (for example, Vav) and kinases (for example, ROCK), has also been shown to have critical roles in linking the activation of chemoattractant receptors to cytoskeletal changes and the formation of lamellipodia and uropods[14]. Rac1 and Cdc42 localize to the leading edge of the cell and regulate the generation of cell protrusions, whereas RhoA localizes to the trailing edge of the migrating cell, where it regulates non-muscle myosins and cell contraction and de-adhesion[14].

Despite the insights noted above, many gaps remain in the understanding of how chemokines and other chemoattractants control this highly integrated multistep process of cell migration. We therefore undertook an RNA-mediated interference (RNAi)-based screen to identify genes previously unknown to be important for chemotaxis. We chose to initially study the effect of gene knockdown on T cell chemotaxis induced by the chemokine CXCL12. CXCL12 and its receptor, CXCR4 (A000636), are essential molecules that direct the migration of essentially all cells, including lymphocytes and hematopoietic stem cells, and are considered to be the primordial chemokine receptor–ligand pair[15,16].

RESULTS

To identify genes and pathways required for chemoattractant-induced chemotaxis, we did a lentivirus-based RNAi screen. As our model system, we examined CXCL12-induced, CXCR4-mediated chemotaxis of lymphocytes. We generated short hairpin RNA (shRNA) molecules expressed from lentiviral vectors based on human immunodeficiency virus type 1 and tested their ability to knock down gene expression in lymphocytes. For this, we coinfected SupT1 cells (a human T cell lymphoma line) with lentivirus expressing an shRNA targeting enhanced green fluorescent protein (eGFP) plus lentivirus expressing eGFP and found that eGFP expression was much lower in those cells than in cells coinfected with lentivirus expressing 'scrambled' shRNA and lentivirus expressing eGFP (Supplementary Fig. 1a).

We then assessed 1,500 arrayed shRNA-encoding viruses obtained from The RNAi Consortium shRNA Library[17], which targeted 300 genes predominantly but not exclusively encoding kinases and phosphatases, as well as lentiviruses encoding shRNA targeting eGFP, for their ability to affect chemotaxis (Fig. 1a; targeted genes, Supplementary Table 1). After infecting and selecting cells, we assessed their ability to migrate to CXCL12 in a Transwell chemotaxis chamber, in a primary screen[18] (Fig. 1a). By secondary screening we confirmed 11 genes that affected CXCL12-induced migration. These included two genes, *SPP1* (encoding osteopontin) and *ZAP70* (encoding the tyrosine kinase Zap70), that have been linked before to chemotaxis[19,20]. Infection with two viruses targeting distinct regions of *SPP1* resulted in less migration of SupT1 cells (Supplementary Fig. 1b, c). The decrease in SupT1 chemotaxis correlated with the decrease in *SPP1* mRNA in infected cells (Supplementary Fig. 1c, d). We also identified nine genes previously unknown to influence chemotaxis; these included genes encoding two members of the synaptotagmin family of calcium-dependent regulators of vesicle fusion: SYT2 (A002560), and a related protein, SYTL5. These data demonstrating that synaptotagmins regulate chemotaxis suggested a requirement for vesicle fusion in cell migration and led us to study the role of synaptotagmins in chemotaxis in more detail.

Infection with virus targeting *SYTL5* mRNA diminished the ability of SupT1 cells to migrate in response to CXCL12 (Fig. 1b). This effect correlated with the ability of the shRNA-encoding virus to diminish *SYTL5* mRNA expression (Supplementary Fig. 2a), which suggested that these results were not due to off-target effects of the shRNA. The knockdown of *SYTL5* had no effect on the proliferation of SupT1 cells (Supplementary Fig. 2b), which demonstrated that the shRNA targeting *SYTL5* was not toxic to the cells. To determine if SYTL5 has a similar role in other cells, we used the virus that knocked down its expression in SupT1 cells to infect THP-1 cells (a human monocytic leukemia cell line). Infection with lentivirus encoding shRNA targeting *SYTL5* diminished the ability of THP-1 cells to migrate in response to CCL2, the ligand for the chemokine receptor CCR2 (Fig. 1c). The decrease in SYTL5 protein abundance in SupT1 and THP-1 cells inhibited chemotaxis to different chemokines, which demonstrated that the requirement for SYTL5 in chemotaxis was not limited to one cell type or to one chemokine–chemokine receptor pair.

We also identified another member of the synaptotagmin family, SYT2, in our initial screen. Decreasing the abundance of *SYT2* mRNA resulted in enhanced migration of SupT1 cells (Fig. 1b) and THP-1 cells (Fig. 1c) in response to chemokines. The enhanced chemotaxis in SupT1 cells correlated with lower abundance of *SYT2* mRNA and SYT2 protein (Fig. 1d–f). These data demonstrate that SYT2 is a negative regulator of chemotaxis, analogous to its known role as a negative regulator of exocytosis in mast cells[21].

We then analyzed 14 additional genes encoding synaptotagmin molecules and synaptotagmin-like molecules for their role in chemotaxis by using shRNA targeting each gene in Transwell chemotaxis assays. Only shRNA targeting *SYT7*, which encodes the lysosomal membrane

protein SYT7 (A002565)[22], a positive regulator of lysosome exocytosis[23], significantly affected the ability of T cells to migrate in response to CXCL12 (Fig. 1b). The efficiency of the knockdown of *SYT7* mRNA correlated with the decrease in the migration of SupT1 cells to CXCL12 (Supplementary Fig. 2c, d). Splenocytes obtained from SYT7-deficient (*Syt7*$^{-/-}$) mice[24] had less ability to migrate in response to CXCL12 than did splenocytes obtained from wild-type mice (Fig. 1g), which confirmed the effect of the *SYT7* knockdown.

Our findings that SYT7, SYT2 and SYTL5 regulate chemotaxis suggested that vesicle fusion and, in particular, lysosome exocytosis are involved in directed cell migration. To further extend that hypothesis, we used RNAi silencing to analyze genes encoding members of the Rab family of small GTPases that regulate the movement of lysosomes to the membrane for their role in chemotaxis. We chose Rab27a (A001978) because it regulates the exocytosis of secretory lysosomes in cytotoxic T lymphocytes[25] and directly interacts with SYTL5 (ref. [26]). We also selected Rab3a because it interacts with synaptotagmin family members and has an important role in regulated exocytosis[27,28]. In cells in which expression of *RAB27A* or *RAB3A* mRNA was targeted by shRNA, chemotaxis to CXCL12 was markedly inhibited (Fig. 2a). The lower chemotaxis in SupT1 cells correlated with the decrease in the abundance of *RAB27A* mRNA and Rab27a protein (Fig. 2b–d). The lower chemotaxis in SupT1 cells similarly correlated with the decrease in *RAB3A* mRNA (Supplementary Fig. 2e). These data demonstrated that the small GTPases Rab27a and Rab3a, proteins known to regulate lysosome exocytosis and interact with synaptotagmins, also have a role in lymphocyte chemotaxis.

To further analyze the migration defect caused by SYT7 deficiency, we obtained bone marrow–derived neutrophils (BMDNs) from *Syt7*$^{-/-}$and wild-type mice and analyzed their ability to migrate in response to the peptide chemoattractant fMLP with a Zigmond chemotaxis chamber[29] and time-lapse video microscopy (Fig. 3 and Supplementary Movies 1 and 2). *Syt7*$^{-/-}$ BMDNs migrated less than half the distance that wild-type BMDNs migrated (Fig. 3a, b). The migration velocity of neutrophils obtained from *Syt7*$^{-/-}$ mice was significantly less than that of wild-type BMDNs (Fig. 3c). The diminished chemotaxis was quantitatively similar to the diminshed membrane repair reported for *Syt7*$^{-/-}$ cells[24]. SYT7 deficiency also adversely affected the directionality of cell migration (Fig. 3d, e). Consistent with those findings, polarized *Syt7*$^{-/-}$ cells had less prominent lamellopodia than those of wild-type cells (Supplementary Movies 1 and 2), and the extent of cell polarization was less during cell migration (Fig. 3f). These data demonstrate that SYT7 is a positive regulator of chemotaxis that affects both velocity and directionality in chemoattractant-induced leukocyte migration.

To extend our observations to the *in vivo* setting, we examined the effect of SYT7 deficiency on the recruitment of neutrophils in a model of gout induced by injection of monosodium urate (MSU) crystals into preformed air pouches on the dorsum of mice[30–32]. At 8 h after injecting PBS or MSU crystals, we lavaged the air pouches and counted recruited cells and determined the frequency of neutrophils ($CD11b^+Ly6C^+$) and monocytes ($CD11b^+Ly6C^-$) by flow cytometry. The percentage (Fig. 4a) and absolute number (Fig. 4b) of neutrophils recruited into the air pouch by MSU crystals were much lower in *Syt7*$^{-/-}$ mice (recruitment index (MSU/PBS), 4.4) than in wild-type mice (recruitment index, 42.8). As expected, the air pouches of wild-type and *Syt7*$^{-/-}$ mice did not have more monocytes (Fig. 4b). However, at 8 h after MSU crystal injection, we recovered fewer monocytes from air pouches of *Syt7*$^{-/-}$ mice, which suggested a recruitment defect for monocytes as well. As this model is dependent on the induction of interleukin 1β (IL-1β) and CXCL2 (MIP-2; ligand for the neutrophil chemokine receptor CXCR2) in resident macrophages, we determined the ability of *Syt7*$^{-/-}$ macrophages to secrete IL-1β and CXCL2 after being activated with MSU crystals. Peritoneal macrophages derived from wild-type and *Syt7*$^{-/-}$ mice showed no difference in their ability to secrete IL-1β or CXCL2 (MIP-2) after being stimulated with MSU crystals (Fig. 4c) or heat-killed *Legionella pneumophilia* (data not shown), which demonstrated that the secretion of IL-1β and

chemokines was not impaired in SYT7-deficient cells (Fig. 4c). Together these data demonstrate that SYT7 is required for chemokine-dependent recruitment of neutrophils *in vivo*.

To begin to explore the mechanism by which synaptotagmin and Rab proteins influence CXCL12-mediated chemotaxis, we determined if knockdown of the genes encoding these molecules affected the surface expression of CXCR4. We infected cell lines with virus expressing shRNA targeting *SYTL5*, *SYT2*, *SYT7*, *RAB27A* or *RAB3A* and assessed CXCR4 surface expression and CXCR4 internalization after stimulation with CXCL12 (Fig. 5a). There was no significant difference between any of the knockdown cell lines or between *Syt7*$^{-/-}$ splenocytes and cells with shRNA-mediated knockdown of eGFP or wild-type cells in their surface expression of CXCR4 (Fig. 5a, b). Similarly, CXCL12-induced CXCR4 internalization was not significantly altered in any of the knockdown cell lines or in *Syt7*$^{-/-}$ cells versus cells with shRNA-mediated knockdown of eGFP or wild-type cells (Fig. 5a, b).

Actin polymerization is also required for effective directional cell migration[33]. We therefore determined if silencing of *SYT7*, *SYTL5*, *SYT2*, *RAB27A* or *RAB3A* affected F-actin polymerization (Fig. 5c). Knockdown of *SYT7*, *SYT2*, *RAB27A* or *RAB3A* mediated by shRNA had a minimal effect on chemoattractant-induced F-actin polymerization, as measured by flow cytometry (Fig. 5c). Splenocytes obtained from *Syt7*$^{-/-}$ mice had F-actin polymerization equivalent to that of cells obtained from wild-type mice after stimulation by CXCL12, which confirmed our data obtained with shRNA-mediated knockdown of *SYT7* (Fig. 5d). In contrast, shRNA-mediated knockdown of *SYTL5* resulted in less F-actin polymerized after CXCL12 stimulation (Fig. 5c). Knockdown of *SYT7*, *SYTL5*, *SYT2* or *RAB27A* also had no significant effect on calcium release after chemokine stimulation (Fig. 5e), which demonstrated that the effects of synaptotagmins on chemotaxis are downstream of calcium release.

Because activation of the small GTPases RhoA, Cdc42 and Rac is also critical for cell migration[14], we studied the effect of SYT7 on chemokine-induced activation of these GTPases. We obtained splenocytes from wild-type and *Syt7*$^{-/-}$ mice and analyzed activated RhoA, Cdc42 and Rac in the cells at rest and at 1, 3, 6 and 12 min after stimulation with CXCL12 (Fig. 5f). CXCL2 induced equivalent activation profiles for these GTPases in cells obtained *Syt7*$^{-/-}$ mice and wild-type mice (Fig. 5f), which demonstrated that SYT7 is not directly involved in GTPase activation after chemokine stimulation.

Synaptotagmin proteins contain calcium-sensing domains that mediate their role in calcium-dependent vesicle fusion[22]. As a transient increase in intracellular free calcium is a hallmark of chemoattractant receptor activation, it is possible that synaptotagmins have a similar role in mediating calcium-dependent vesicle fusion after chemo-attractant stimulation, which may also be required for chemotaxis. To begin to test this, we first studied the effect of the intracellular calcium chelator BAPTA on chemokine-induced calcium flux and chemotaxis. As expected, BAPTA blocked calcium influx after chemokine stimulation (Fig. 5e). BAPTA also completely inhibited the migration of SupT1 cells and Jurkat cells (a human T cell leukemia line) to CXCL12 (Fig. 6a and Supplementary Fig. 3a). In contrast, BAPTA had no effect on chemokine-induced polymerization of F-actin (Fig. 6b and Supplementary Fig. 3b), which suggested that an increase in intracellular free calcium is required for chemotaxis but is not required for F-actin polymerization.

SYT7 (ref. [22]) and Rab27a[34] are known positive regulators of lysosome exocytosis, whereas SYT2 (ref. [21]) is a known negative regulator of lysosome exocytosis. We therefore investigated whether stimulation with chemoattractants induced calcium-dependent lysosome fusion and exocytosis. To determine if stimulation with chemoattractants results in the fusion of lysosomes with the cell membrane, we analyzed expression of the lysosomal marker LAMP-1 on the

surface of BMDNs after stimulation with the chemoattractant C5a (Fig. 6c). Cell-surface expression of LAMP-1 was markedly enhanced after C5a stimulation (Fig. 6c). Consistent with those findings, extracellular β-hexosaminidase activity increased after the addition of fMLP to HL-60 human promyelocytic leukemia cells (Supplementary Fig. 4), which demonstrated that chemoattractants induce lysosome–cell membrane fusion that results in the release of lysosomal contents into the extracellular milieu. Similar to its effect on chemotaxis, BAPTA resulted in much lower chemoattractant-induced expression of LAMP-1 on the cell surface (Fig. 6c). These data demonstrate that chemoattractant stimulation results in calcium-dependent fusion of LAMP-1^+ vesicles with the cell membrane.

We next tested the effect of SYT7 deficiency on chemoattractant-induced cell surface expression of LAMP-1. Neutrophils derived from wild-type and *Syt7*$^{-/-}$ mice had similar basal surface expression of LAMP-1 (Fig. 6d). However, the induction of cell surface expression of LAMP-1 after C5a stimulation was markedly attenuated in *Syt7*$^{-/-}$ neutrophils compared with that in wild-type neutrophils (Fig. 6d). To localize chemokine-induced lysosome fusion, we imaged podocytes, which are 40 times larger than leukocytes. Podocytes express the chemokine receptor CXCR3 (ref. [35]) and have been shown to migrate in response to chemokines[36]. We stimulated podocytes with the CXCR3 ligand CXCL11 and found that the lysosomal markers cathepsin-L and LAMP-2 localized to the plasma membrane (Fig. 6e), which demonstrated again that chemokine stimulation results in the fusion of lysosomes with the cell membrane. Together these data suggest that synaptotagmins function downstream of chemoattractant-induced calcium release and upstream of the fusion of LAMP-1^+ vesicles with the plasma membrane.

To visualize the role of SYT7 in vesicle localization during chemotaxis, we used laser-scanning confocal microscopy to analyze activated wild-type and *Syt7*$^{-/-}$ $CD4^+$ T cells migrating in a CXCL10 gradient (Fig. 7a). We used the red fluorescent dye LysoTracker Red to visualize intracellular vesicles with a low pH, including lysosomes. Migrating *Syt7*$^{-/-}$ T cells had much more accumulation of LysoTracker Red in the distal ends of their uropods (Fig. 7a and Supplementary Movies 3–6). To quantify the accumulation of LysoTracker Red, we sampled fluorescence intensity of cell bodies and uropods of polarized cells and then normalized those results to cell area. The cell bodies of polarized wild-type and *Syt7*$^{-/-}$ lymphocytes had a similar area, whereas the uropods of *Syt7*$^{-/-}$ lymphocytes were marginally smaller than those of wild-type lymphocytes (Fig. 7b). *Syt7*$^{-/-}$ T cells showed twofold greater LysoTracker Red fluorescence across the cell body and over fourfold greater normalized intensity in the uropod than that of wild-type cells (Fig. 7c). The accumulation of LysoTracker Red–stained vesicles in *Syt7*$^{-/-}$ lymphocytes is consistent with less fusion of these vesicles with the cell membrane than that of migrating wild-type lymphocytes. In addition, the ratio of uropod to cell-body fluorescence intensity was twice as high in polarized *Syt7*$^{-/-}$ cells as in polarized wild-type cells (Fig. 7d), which demonstrated that LysoTracker Red–stained vesicles were distributed differently in *Syt7*$^{-/-}$ cells exposed to a chemokine gradient.

Coincident with the accumulation of LysoTracker Red described above, uropods in *Syt7*$^{-/-}$ T cells seemed to have difficulty releasing from the substrate, which resulted in cells that seemed to be stuck in place by a tethered tail (Fig. 7e and Supplementary Movies 3–6). Over the 30 min of observation, 6.14% of polarized wild-type T cells (7 of 114) demonstrated an adherent phenotype, whereas 81.48% of polarized *Syt7*$^{-/-}$ T cells (88 of 108) demonstrated an adherent phenotype (Fig. 7f). Furthermore, comparison of the average time of adherence of wild-type and *Syt7*$^{-/-}$ T cells with the adherent phenotype at their uropods showed that *Syt7*$^{-/-}$ T cells had an average adherence time of 29.43 ± 0.36 min, whereas for the wild-type cells it was 20.46 ± 3.76 min (Fig. 7g). Thus, the few wild-type T cells with the adhesion phenotype had a shorter duration period of adhesion, whereas the majority of *Syt7*$^{-/-}$ T cells remained adherent at their uropods for the duration of the 30-minute observation period. The phenotype we

observed for the impaired migration of *Syt7*$^{-/-}$ neutrophils and T cells suggests a previously unknown role for synaptogamins and calcium-dependent vesicle fusion in the de-adhesion process required for cell migration.

DISCUSSION

In an RNAi-based genetic screen to identify genes encoding molecules that function in leukocyte chemotaxis, we have identified genes encoding molecules known to regulate vesicle trafficking and fusion. We found that three genes in the synaptotagmin family encoding calcium-sensing membrane proteins regulated chemoattractant-induced directed cell migration. We identified SYT7 and the related protein SYTL5 as positive regulators of chemotaxis, whereas we found SYT2 to be a negative regulator of chemotaxis. Those findings are consistent with the opposing roles of these proteins in regulating calcium-dependent lysosomal exocytosis[21,22]. We also identified Rab27a and Rab3a, small GTPases that regulate lysosome transport and interact with the synaptotagmin proteins identified[37], as positive regulators of chemotaxis. We used SYT7-deficient mice to further characterize the role of SYT7 in cell migration. Neutrophils derived from those mice migrated more slowly and with less directionality than did neutrophils derived from wild-type mice. Furthermore, SYT7-deficient mice showed a neutrophil recruitment defect in an *in vivo* model of MSU crystal–induced gout, even though SYT7-deficient and wild-type macrophages secreted equivalent amounts of IL-1β and CXCL12 (MIP-2) in response to MSU crystals. Exploring the mechanism by which synaptotagmins influence chemotaxis, we found that SYT7 as well as calcium flux were required for chemoattractant-induced cell surface expression of LAMP-1. By confocal video imaging of lymphocytes migrating in a chemokine gradient, we observed that LysoTracker Red–stained vesicles accumulated in the uropods of the SYT7-deficient cells, which also suggested that SYT7 mediates chemokine-induced fusion of lysosomes with the cell membrane in migrating cells. Furthermore, we found that SYT7 was required for effective de-adhesion and uropod detachment. Collectively, our data identify a molecular pathway required for chemotaxis mediated by synaptotagmins and Rab proteins that involves chemoattractant-induced vesicle exocytosis and uropod release.

The idea that membrane flow and vesicle trafficking have a role in cell migration has been considered for many years. In 1962 it was suggested that there is a membrane cycle during cell migration; experiments showed that 100-nM beads move around the cell surface during cell migration[38]. Later it was shown that membrane flows toward the rear of the migrating cell and caps at the front of the cell[39–41]. In 1983 further evidence for vesicle trafficking during cell migration was presented showing that the surface of the HeLa human cervical cancer cell becomes rough during cell movement, thus suggesting membrane recycling[42]. Subsequently, it has been shown that lipids move to the front, whereas proteins move to the rear, of migrating cells[43]. Consistent with that, in 1994 it was shown that recycling receptors in endocytic vesicles are routed to the plasma membrane of the leading lamella of migrating chick fibroblasts[44]. These descriptive studies all suggested that vesicle trafficking occurs during cell migration, but they did not explore the molecular mechanisms that mediate this process or demonstrate the functional importance of vesicle trafficking in cell migration. We have now done both by defining a role for several proteins (SYT7, SYTL5, SYT2, Rab27a and Rab3a) in a pathway that controls vesicle trafficking in chemotaxis and, using STY7-deficient mice, we have demonstrated that this process is important for chemotaxis *in vitro* and for cell migration *in vivo*.

Exploring the mechanism by which synaptotagmin and Rab proteins influence chemotaxis, we found that chemokine receptor abundance and chemokine-induced receptor internalization were not affected by knockdown of *SYT7*, *SYTL5*, *SYT2*, *RAB27A* or *RAB3A*. Our findings differ from those of a study that found that another synaptotagmin, SYT3, regulates recycling

and surface expression of CXCR4 in the TAM2D2 mouse T cell line[45]. This suggests that the role of SYT3 may be different from that of the synaptotagmins identified in our study. In addition, we also found that chemokine-induced polymerization of F-actin and calcium flux were not affected by knockdown of *SYT7*, *SYT2*, *RAB27A* or *RAB3A*. Knockdown of *SYTL5*, however, resulted in less F-actin polymerization after chemokine stimulation, which suggests that this synaptotagmin-like protein may have an effect on cells distinct from that of the other synaptotagmins studied. Together these findings suggested that synaptotagmins participate in chemotaxis downstream of the expression of chemo-attractant receptors and initial signal transduction. Given the known function of synaptotagmins in mediating calcium-induced fusion of vesicles with the cell membrane, we suspected that synaptotagmins may have a similar role in chemoattractant-induced chemotaxis.

$Ins(1,4,5)P_3$, generated via chemoattractant receptor activation of PLC, is thought to induce the increase in intracellular free calcium by activating $Ins(1,4,5)P_3$ receptors on the endoplasmic reticulum, which then open up calcium channels, resulting in the release of free calcium into the cytoplasm. In migrating cells, calcium is thought to contribute to many processes, including directional sensing, cytoskeleton redistribution (through effects on myosin light-chain kinase or calmodulin kinase, among others), traction force regeneration and the relocation of focal adhesions[3,4,9,10]. Additionally, it has been suggested that calcium is important for uropod release in migrating neutrophils[46]. However, an absolute requirement for calcium flux in cell migration has been controversial. PLC-β2 and PLC-β3 are the two main PLC isoforms found in leukocytes, and neutrophils obtained from mice doubly deficient in PLC-β2 and PLC-β3 have a blunted calcium flux and enhanced migration compared with that of wild-type neutrophils, which suggests that calcium may not be required for chemotaxis[47]. In contrast, lymphocytes obtained from mice doubly deficient in PLC-β2 and PLC-β3 have no calcium flux and much less chemotaxis[48], which suggests that PLC-β2 and PLC-β3 are required for calcium flux and chemotaxis in lymphocytes but not in neutrophils, in which other PLC isoforms may also contribute to localized calcium influx and chemotaxis. Similar to results obtained in our experiments with BAPTA, lymphocyte chemotaxis has been shown to be inhibited by calcium chelation[48]. Notably, we found that calcium chelation also inhibited the chemotaxis of Jurkat T cells, even though a detectable calcium flux is not typically evident in these cells after chemokine stimulation. It is likely that calcium is required at specific intracellular microdomains during chemotaxis[49] that may not always be appreciated in a whole-cell calcium-efflux assay.

As mentioned above, the identification of synaptotagmin family members in our RNAi screen suggested that chemokine-induced release of calcium may induce the fusion of vesicles with the cell membrane and this may in turn be required for effective chemotaxis. Synaptotagmin family members, including SYT7, SYT2 and SYTL5, contain calcium-sensing domains that are critical for the regulation of calcium-induced vesicle fusion[23]. We therefore sought to determine if chemoattractant-induced calcium flux has a role in synaptotagmin-mediated vesicle fusion during chemotaxis. In support of our hypothesis, we found that chemoattractants induced cell surface expression of LAMP-1, which suggested that chemoattractant receptor signaling can induce the fusion of lysosomes with the cell surface. We also found that this process required both calcium and SYT7, which suggests that calcium-induced vesicle fusion contributes to effective chemotaxis. This result is consistent with the observation that VAMP-7, a SYT7-regulated SNARE protein required for calcium-dependent fusion of lysosomes with the cell membrane, has a role in epithelial cell migration[50].

We also used live-cell video microscopy of LysoTracker Red–labeled wild-type and SYT7-deficient lymphocytes migrating in a chemokine gradient to visualize the movement of lysosomes in migrating lymphocytes. Although we were unable to visualize the movement of individual vesicles with this technique, we found that LysoTracker Red–stained vesicles

accumulated to a greater extent in the uropods of SYT7-deficient cells than in those of wild-type cells. This phenotype was consistent with the failure of lysosome–cell membrane fusion in SYT7-deficient cells. We also unexpectedly found that SYT7-deficient cells had difficulty releasing uropods and had prolonged attachment to the substrate. This phenotype was reminiscent of that of neutrophils treated with a calcium chelator[46]. Uropod release and de-adhesion are active regulated processes required for effective cell migration. De-adhesion is a calcium-dependent process that requires activity of the RhoA kinase ROCK and nonmuscle myosin heavy chain IIA in the uropod[46,51–53]. Our data suggest that SYT7-dependent fusion of intracellular vesicles with the cell membrane may be required for the delivery of cargo important for the detachment of uropods from the substrate. The delivered cargo may be proteins known to accumulate in the uropods of migrating cells or phospholipids required for the cell membrane dynamics associated with uropod release. The identification of these factors awaits further investigation.

Of potential clinical relevance to our study, Chediak-Higashi syndrome is a congenital immunodeficiency that results from a mutation in *LYST* (encoding the lysosomal trafficking regulator LYST)[54]. Neutrophils obtained from patients with this syndrome have impaired function, including defective chemotaxis. Our study raises the possibility that the impaired neutrophil chemotaxis seen in Chediak-Higashi syndrome may be a direct consequence of a defect in lysosomal transport. Our data showing that SYT7-deficient cells had impaired chemotaxis *ex vivo* and cell migration *in vivo* demonstrate that chemokine-induced vesicle transport and fusion pathways are important in leukocyte migration.

METHODS

Methods and any associated references are available in the online version of the paper at http://www.nature.com/natureimmunology/.

Supplementary Material

Refer to Web version on PubMed Central for supplementary material.

Acknowledgments

We thank the Immune Circuits and RNAi Platform groups of the Broad Institute and W. Xu for discussions and the Imaging Core of the Ragon Institute of MGH, MIT and Harvard. Supported by the US National Institutes of Health (R01 DK074449 to A.D.L. and R01 GM064625 to N.W.A.), the Defense Advanced Research Projects Agency (W81XWH-04-C-0139 to N.H.), Fundação Luso-Americana para o Desenvolvimento (L.F.M.) and Fundação para a Ciência e a Tecnologia (L.F.M.).

References

1. Viola A, Luster AD. Chemokines and their receptors: drug targets in immunity and inflammation. Annu Rev Pharmacol Toxicol 2008;48:171–197. [PubMed: 17883327]
2. Murphy PM. The molecular biology of leukocyte chemoattractant receptors. Annu Rev Immunol 1994;12:593–633. [PubMed: 8011292]
3. Ridley AJ, et al. Cell migration: integrating signals from front to back. Science 2003;302:1704–1709. [PubMed: 14657486]
4. Van Haastert PJ, Devreotes PN. Chemotaxis: signalling the way forward. Nat Rev Mol Cell Biol 2004;5:626–634. [PubMed: 15366706]
5. Kehrl JH, Hwang IY, Park C. Chemoattract receptor signaling and its role in lymphocyte motility and trafficking. Curr Top Microbiol Immunol 2009;334:107–127. [PubMed: 19521683]
6. Wu D, LaRosa GJ, Simon MI. G protein-coupled signal transduction pathways for interleukin-8. Science 1993;261:101–103. [PubMed: 8316840]

7. Malchow D, Bohme R, Rahmsdorf HJ. Regulation of phosphorylation of myosin heavy chain during the chemotactic response of Dictyostelium cells. Eur J Biochem 1981;117:213–218. [PubMed: 7262086]
8. Liu G, Newell PC. Regulation of myosin regulatory light chain phosphorylation via cyclic GMP during chemotaxis of Dictyostelium. J Cell Sci 1994;107:1737–1743. [PubMed: 7983143]
9. Pettit EJ, Fay FS. Cytosolic free calcium and the cytoskeleton in the control of leukocyte chemotaxis. Physiol Rev 1998;78:949–967. [PubMed: 9790567]
10. Brundage RA, Fogarty KE, Tuft RA, Fay FS. Calcium gradients underlying polarization and chemotaxis of eosinophils. Science 1991;254:703–706. [PubMed: 1948048]
11. Stoyanov B, et al. Cloning and characterization of a G protein-activated human phosphoinositide-3 kinase. Science 1995;269:690–693. [PubMed: 7624799]
12. Stephens L, et al. A novel phosphoinositide 3 kinase activity in myeloid-derived cells is activated by G protein βγ subunits. Cell 1994;77:83–93. [PubMed: 8156600]
13. Hannigan MO, Huang CK, Wu DQ. Roles of PI3K in neutrophil function. Curr Top Microbiol Immunol 2004;282:165–175. [PubMed: 14594217]
14. Thelen M, Stein JV. How chemokines invite leukocytes to dance. Nat Immunol 2008;9:953–959. [PubMed: 18711432]
15. Zou YR, Kottmann AH, Kuroda M, Taniuchi I, Littman DR. Function of the chemokine receptor CXCR4 in haematopoiesis and in cerebellar development. Nature 1998;393:595–599. [PubMed: 9634238]
16. Ma Q, et al. Impaired B-lymphopoiesis, myelopoiesis, and derailed cerebellar neuron migration in CXCR4- and SDF-1-deficient mice. Proc Natl Acad Sci USA 1998;95:9448–9453. [PubMed: 9689100]
17. Root DD, Hacohen N, Hahn WC, Lander ES, Sabatini DM. Genome-scale loss-of-function screening with a lentiviral RNAi library. Nat Methods 2006;3:715–719. [PubMed: 16929317]
18. Colvin RA, Campanella GS, Sun J, Luster AD. Intracellular domains of CXCR3 that mediate CXCL9, CXCL10, and CXCL11 function. J Biol Chem 2004;279:30219–30227. [PubMed: 15150261]
19. Koh A, et al. Role of osteopontin in neutrophil function. Immunology 2007;122:466–475. [PubMed: 17680800]
20. Ticchioni M, et al. Signaling through ZAP-70 is required for CXCL12-mediated T-cell transendothelial migration. Blood 2002;99:3111–3118. [PubMed: 11964272]
21. Baram D, et al. Synaptotagmin II negatively regulates Ca^{2+}-triggered exocytosis of lysosomes in mast cells. J Exp Med 1999;189:1649–1658. [PubMed: 10330444]
22. Martinez I, et al. Synaptotagmin VII regulates Ca^{2+}-dependent exocytosis of lysosomes in fibroblasts. J Cell Biol 2000;148:1141–1149. [PubMed: 10725327]
23. Reddy A, Caler EV, Andrews NW. Plasma membrane repair is mediated by Ca^{2+}-regulated exocytosis of lysosomes. Cell 2001;106:157–169. [PubMed: 11511344]
24. Chakrabarti S, et al. Impaired membrane resealing and autoimmune myositis in synaptotagmin VII-deficient mice. J Cell Biol 2003;162:543–549. [PubMed: 12925704]
25. Stinchcombe JC, et al. Rab27^{a} is required for regulated secretion in cytotoxic T lymphocytes. J Cell Biol 2001;152:825–834. [PubMed: 11266472]
26. Kuroda TS, Fukuda M, Ariga H, Mikoshiba K. Synaptotagmin-like protein 5: a novel Rab27A effector with C-terminal tandem C2 domains. Biochem Biophys Res Commun 2002;293:899–906. [PubMed: 12051743]
27. Coppola T, et al. Direct interaction of the Rab3 effector RIM with Ca^{2+} channels, SNAP-25, and synaptotagmin. J Biol Chem 2001;276:32756–32762. [PubMed: 11438518]
28. Geppert M, Goda Y, Stevens CF, Sudhof TC. The small GTP-binding protein Rab3A regulates a late step in synaptic vesicle fusion. Nature 1997;387:810–814. [PubMed: 9194562]
29. Zigmond SH. Orientation chamber in chemotaxis. Methods Enzymol 1988;162:65–72. [PubMed: 3067054]
30. Chen CJ, et al. MyD88-dependent IL-1 receptor signaling is essential for gouty inflammation stimulated by monosodium urate crystals. J Clin Invest 2006;116:2262–2271. [PubMed: 16886064]

31. Martin WJ, Walton M, Harper J. Resident macrophages initiating and driving inflammation in a monosodium urate monohydrate crystal-induced murine peritoneal model of acute gout. Arthritis Rheum 2009;60:281–289. [PubMed: 19116939]
32. Terkeltaub R, Baird S, Sears P, Santiago R, Boisvert W. The murine homolog of the interleukin-8 receptor CXCR-2 is essential for the occurrence of neutrophilic inflammation in the air pouch model of acute urate crystal-induced gouty synovitis. Arthritis Rheum 1998;41:900–909. [PubMed: 9588743]
33. Manes S, et al. Mastering time and space: immune cell polarization and chemotaxis. Semin Immunol 2005;17:77–86. [PubMed: 15582490]
34. Izumi T. Physiological roles of Rab27 effectors in regulated exocytosis. Endocr J 2007;54:649–657. [PubMed: 17664848]
35. Huber TB, et al. Expression of functional CCR and CXCR chemokine receptors in podocytes. J Immunol 2002;168:6244–6252. [PubMed: 12055238]
36. Burt D, et al. The monocyte chemoattractant protein-1/cognate CC chemokine receptor 2 system affects cell motility in cultured human podocytes. Am J Pathol 2007;171:1789–1799. [PubMed: 18055544]
37. Fukuda M. Versatile role of Rab27 in membrane trafficking: focus on the Rab27 effector families. J Biochem 2005;137:9–16. [PubMed: 15713878]
38. Marcus PI. Dynamics of surface modification in myxovirus-infected cells. Cold Spring Harb Symp Quant Biol 1962;27:351–365. [PubMed: 13932922]
39. Abercrombie M, Heaysman JE, Pegrum SM. The locomotion of fibroblasts in culture. II RRuffling. Exp Cell Res 1970;60:437–444. [PubMed: 5463639]
40. Abercrombie M, Heaysman JE, Pegrum SM. The locomotion of fibroblasts in culture. I Movements of the leading edge. Exp Cell Res 1970;59:393–398. [PubMed: 4907703]
41. Abercrombie M, Heaysman JE, Pegrum SM. The locomotion of fibroblasts in culture. 3 Movements of particles on the dorsal surface of the leading lamella. Exp Cell Res 1970;62:389–398. [PubMed: 5531377]
42. Bretscher MS, Thomson JN. Distribution of ferritin receptors and coated pits on giant HeLa cells. EMBO J 1983;2:599–603. [PubMed: 6138252]
43. Lee J, Gustafsson M, Magnusson KE, Jacobson K. The direction of membrane lipid flow in locomoting polymorphonuclear leukocytes. Science 1990;247:1229–1233. [PubMed: 2315695]
44. Hopkins CR, Gibson A, Shipman M, Strickland DK, Trowbridge IS. In migrating fibroblasts, recycling receptors are concentrated in narrow tubules in the pericentriolar area, and then routed to the plasma membrane of the leading lamella. J Cell Biol 1994;125:1265–1274. [PubMed: 7515888]
45. Masztalerz A, et al. Synaptotagmin 3 deficiency in T cells impairs recycling of the chemokine receptor CXCR4 and thereby inhibits CXCL12 chemokine-induced migration. J Cell Sci 2007;120:219–228. [PubMed: 17179206]
46. Lawson MA, Maxfield FR. Ca^{2+}- and calcineurin-dependent recycling of an integrin to the front of migrating neutrophils. Nature 1995;377:75–79. [PubMed: 7544874]
47. Li Z, et al. Roles of PLC-β2 and -β3 and PI3Kγ in chemoattractant-mediated signal transduction. Science 2000;287:1046–1049. [PubMed: 10669417]
48. Bach TL, et al. Phospholipase cβ is critical for T cell chemotaxis. J Immunol 2007;179:2223–2227. [PubMed: 17675482]
49. Wei C, et al. Calcium flickers steer cell migration. Nature 2009;457:901–905. [PubMed: 19118385]
50. Proux-Gillardeaux V, Raposo G, Irinopoulou T, Galli T. Expression of the Longin domain of TI-VAMP impairs lysosomal secretion and epithelial cell migration. Biol Cell 2007;99:261–271. [PubMed: 17288539]
51. Yoshinaga-Ohara N, Takahashi A, Uchiyama T, Sasada M. Spatiotemporal regulation of moesin phosphorylation and rear release by Rho and serine/threonine phosphatase during neutrophil migration. Exp Cell Res 2002;278:112–122. [PubMed: 12126963]
52. Lokuta MA, et al. Type Iγ PIP kinase is a novel uropod component that regulates rear retraction during neutrophil chemotaxis. Mol Biol Cell 2007;18:5069–5080. [PubMed: 17928408]

53. Morin NA, et al. Nonmuscle myosin heavy chain IIA mediates integrin LFA-1 de-adhesion during T lymphocyte migration. J Exp Med 2008;205:195–205. [PubMed: 18195072]

54. Introne W, Boissy RE, Gahl WA. Clinical, molecular, and cell biological aspects of Chediak-Higashi syndrome. Mol Genet Metab 1999;68:283–303. [PubMed: 10527680]

55. Mundel P, et al. Rearrangements of the cytoskeleton and cell contacts induce process formation during differentiation of conditionally immortalized mouse podocyte cell lines. Exp Cell Res 1997;236:248–258. [PubMed: 9344605]

56. Kim ND, Chou RC, Seung E, Tager AM, Luster AD. A unique requirement for the leukotriene B4 receptor BLT1 for neutrophil recruitment in inflammatory arthritis. J Exp Med 2006;203:829–835. [PubMed: 16567386]

57. Moffat J, et al. A lentiviral RNAi library for human and mouse genes applied to an arrayed viral high-content screen. Cell 2006;124:1283–1298. [PubMed: 16564017]

58. Naldini L, et al. In vivo gene delivery and stable transduction of nondividing cells by a lentiviral vector. Science 1996;272:263–267. [PubMed: 8602510]

59. Wang X, Seed BA. PCR primer bank for quantitative gene expression analysis. Nucleic Acids Res 2003;31:e154. [PubMed: 14654707]

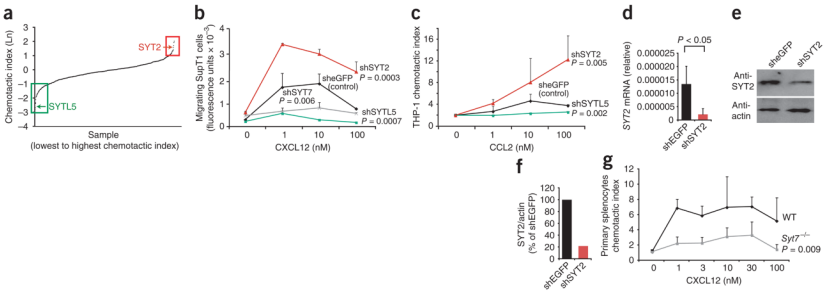

Figure 1.

Screen of chemotaxis by shRNA identifies synaptotagmins SYT2, SYTL5 and SYT7. (**a**) Primary chemotaxis screen showing the chemotactic indices of SupT1 cells infected with 1,500 arrayed lentiviruses encoding shRNA targeting 300 genes. Horizontal axis, individual samples; vertical axis, natural logarithm (Ln) of the chemotactic index; boxes outline results for cells infected with viruses targeting genes selected as putative positive (green) or negative (red) regulators of chemotaxis. (**b**) Transwell chemotaxis of SupT1 cells infected with viruses containing shRNA targeting genes encoding eGFP (sheGFP), SYTL5 (shSYTL5), SYT2 (shSYT2) or SYT7 (shSYT7). (**c**) Transwell chemotaxis of THP-1 cells infected with viruses targeting genes encoding eGFP, SYTL5 or SYT2. (**d**) Quantitative PCR analysis of *SYT2* mRNA abundance in SupT1 cells infected with viruses targeting genes encoding eGFP or SYT2, presented relative to the abundance of *GAPDH* mRNA (encoding glyceraldehyde phosphate dehydrogenase). (**e**) Immmunoblot analysis of extracts from SupT1 cells infected with lentiviruses targeting genes encoding eGFP or SYT2, probed with antibody to SYT2 (anti-SYT2; top) or anti-β-actin (bottom). (**f**) Quantification of SYT2 protein. (**g**) Transwell chemotaxis of wild-type (WT) and $Syt7^{-/-}$ primary splenocytes. *P* values, two-way analysis of variance (ANOVA). Data are representative of an experiment done once (**a**) or experiments done three times (**b**, **c**, **g**; mean and s.e.m. of two samples), at least four times in duplicate (**d**; error bars, s.e.m.) or twice (**e**, **f**).

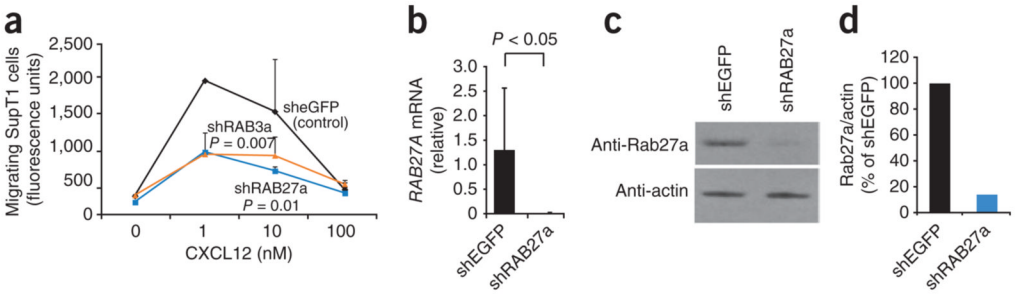

Figure 2.

Knockdown of *RAB27A* and *RAB3A* inhibits T cell chemotaxis. (**a**) Transwell chemotaxis of SupT1 cells infected with viruses targeting genes encoding eGFP, Rab27a or Rab3a. (**b**) Quantitative PCR analysis of *RAB27A* mRNA abundance in SupT1 cells infected with viruses targeting genes encoding eGFP or Rab27a, presented relative to *GAPDH* mRNA abundance. (**c**) Immunoblot analysis of extracts of SupT1 cells infected with lentiviruses targeting genes encoding eGFP or Rab27a, probed with anti-Rab27a (top) or anti-β-actin (bottom). (**d**) Quantification of Rab27a protein, presented as the ratio of the Rab27a to β-actin in lysates of cells infected with lentivirus targeting *RAB27A*, normalized to the ratio in lysates of cells infected with lentivirus targeting the gene encoding eGFP. *P* values, two-way ANOVA (**a**) or Student's *t*-test (**b**). Data are representative of at least three similar experiments (**a**; mean and s.e.m. of two samples) or experiments done at least four times (**b**; error bar, s.e.m.) or twice (**c**, **d**).

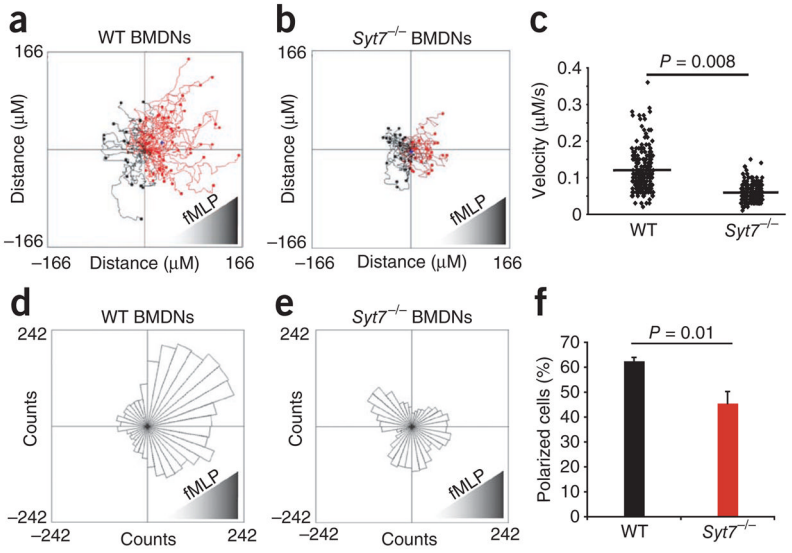

Figure 3.

Migration of wild-type and SYT7-deficient neutrophils *ex vivo*. (**a**, **b**) Tracks of neutrophil migration, derived from stacks of images taken every 15 s for 30 min during migration in a Zigmond chamber in a gradient of fMLP. Data are representative of four similar experiments. (**c**) Migration velocity of wild-type and *Syt7*$^{-/-}$ BMDNs. Each symbol represents an individual cell; small horizontal lines indicate the mean. Data are compiled from four separate experiments. (**d**,**e**) Migration vectors, presented as Rose plots of data obtained in **a**,**b**. *P* = 0.00002 (**d**) or 0.7 (**e**; Rayleigh test for both). Data are representative of four similar experiments. (**f**) Frequency of polarized cells 25 min after exposure to an fMLP gradient (*n* = 100 cells examined at 25 min and categorized as polarized or unpolarized). *P* values, Student's *t*-test. Data are compiled from four similar experiments (error bars, s.e.m.).

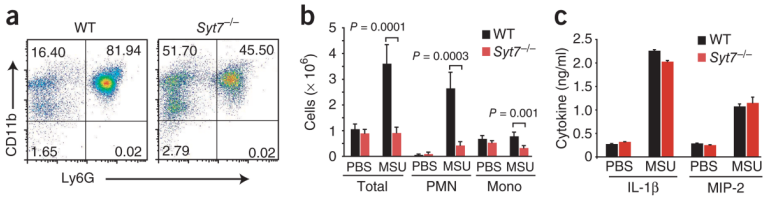

Figure 4.

Migration of wild-type and SYT7-deficient neutrophils *in vivo* in a model of gout. (**a**) Flow cytometry of cells recruited into the air pouch of a wild-type mouse and a *Syt7*$^{-/-}$ mouse injected with MSU crystals; cells were stained with anti-Ly6G and anti-CD11b. Numbers in quadrants indicate percent cells in each. (**b**) Total cells, neutrophils (PMN; CD11b^{+}Ly6C^{+}) and monocytes (Mono; CD11b^{+}Ly6C^{-}) recruited into the air pouches of wild-type mice (n = 11) and *Syt7*$^{-/-}$ mice (n = 11) injected with MSU crystals or wild-type mice (n = 6) and *Syt7*$^{-/-}$ mice (n =6) injected with PBS (control). *P* values, Student's *t*-test. (**c**) Enzyme-linked immunosorbent assay of IL-1β and CXCL2 (MIP-2) in supernatants of wild-type and *Syt7*$^{-/-}$ thioglycolate-recruited peritoneal macrophages primed with lipopolysaccharide, then stimulated with PBS or MSU crystals. No significant difference, wild-type versus *Syt7*$^{-/-}$ (Student's *t*-test). Data are representative of three (**a**,**b**) or two (**c**) experiments (error bars, s.e.m.).

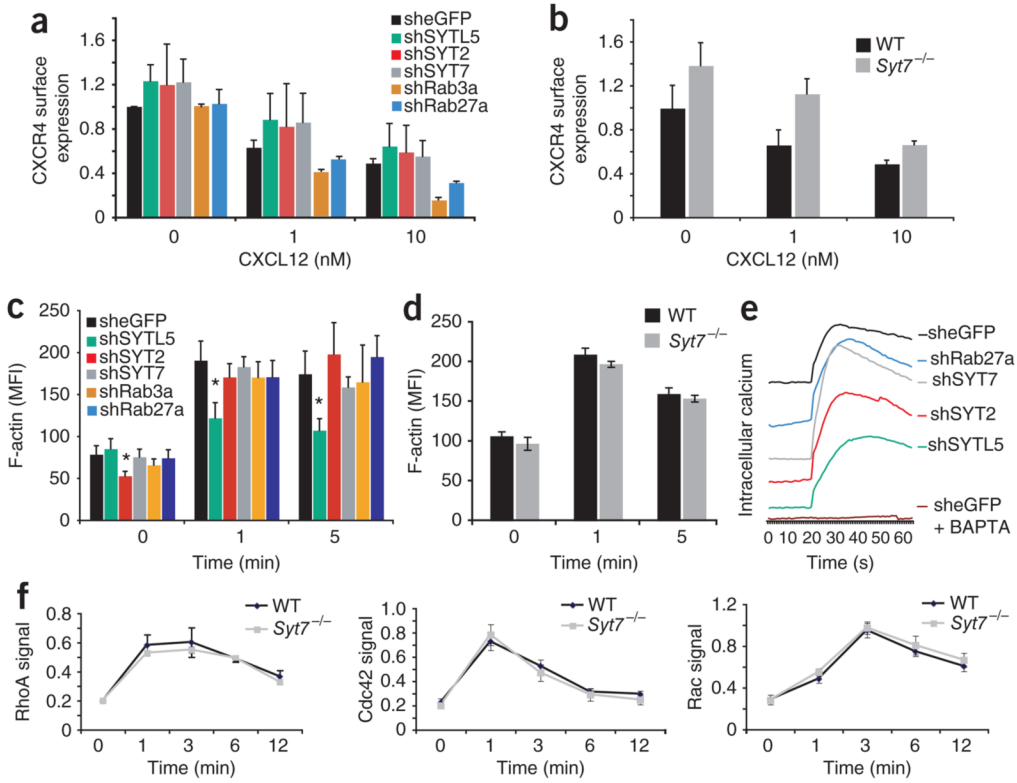

Figure 5.

CXCR4 cell surface expression and chemokine-induced F-actin polymerization and calcium release. (**a**) Cell surface expression of CXCR4 on shRNA-expressing SupT1 cells (key) stimulated with CXCL12 (concentration, horizontal axis). Differences not significant (Student's *t*-test). (**b**) Cell surface expression of CXCR4 on wild-type and *Syt7*$^{-/-}$ splenocytes stimulated with CXCL12 (concentration, horizontal axis), analyzed by flow cytometry. Differences not significant (Student's *t*-test). (**c**) F-actin polymerization in shRNA-expressing SupT1 cells (key) stimulated for various time (horizontal axis) with CXCL12, analyzed by flow cytometry. *$P < 0.02$, versus cells expressing shRNA targeting the gene encoding eGFP at the same time point (Student's *t*-test). (**d**) Flow cytometry of F-actin content in wild-type splenocytes ($n = 3$ mice) and *Syt7*$^{-/-}$ splenocytes ($n = 3$ mice) after stimulation with CXCL12 for various times (horizontal axis). (**e**) Calcium flux in SupT1 cells infected with shRNA-expressing lentivirus (right margin), loaded with the fluorescent calcium indicator Fluo-8 and activated with 10 nM CXCL12, presented as emission at 520 nM after activation at 480 nM; curves were displaced on the vertical axis for clarity. Baselines of original curves were similar (data not shown). (**f**) GTP-bound RhoA, Cdc42, and Rac in cytoplasmic extracts of wild-type and *Syt7*$^{-/-}$ splenocytes stimulated for various times (horizontal axis) with 10 nM CXCL12. No significant difference, wild type versus *Syt7*$^{-/-}$ (Student's *t*-test). Data represent one of three similar experiments (**a**, **b**; average and s.e.m. of two samples), at least three experiments (**c**; average and s.e.m. of two or three replicates of one to four per gene), an experiment done three times (**d**; error bars, s.e.m.) or experiments done in triplicate and repeated three times (**e**), or are representative of three experiments (**e**) or an experiment done in triplicate two times (**f**; error bars, s.e.m.).

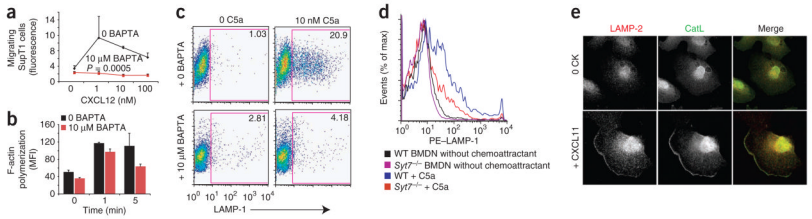

Figure 6.

Effect of calcium on chemotaxis, F-actin polymerization, and chemokine-induced expression of LAMP-1. (**a**) Transwell chemotaxis of SupT1 cells toward CXCL12 with and without (0) treatment with 10 μM BAPTA. *P* value, two-way ANOVA. Data are representative of three similar experiments (mean and s.e.m. of three samples). (**b**) F-actin polymerization with and without treatment with 10 μM BAPTA. Results not significant (Student's *t*-test). Data are from one of three similar experiments (average and s.e.m. of two samples). (**c**) Flow cytometry analysis of the cell surface expression of LAMP-1 on wild-type BMDNs the presence (right) or absence (left) of C5a stimulation (10 nM), with or without BAPTA treatment (left margin). Numbers in outlined areas indicate percent LAMP-1^{+} cells. Data are representative of three experiments done in triplicate. (**d**) Flow cytometry analysis of the cell surface expression of LAMP-1 on wild-type and *Syt7*$^{-/-}$ BMDNs at baseline (without chemoattractant) and after C5a stimulation (+ C5a). Data are representative of three experiments done in triplicate. (**e**) Laser-scanning confocal microscopy of the localization of LAMP-2 and cathepsin-L (CatL) in the podocyte cell membrane before (0 CK; top row) and after (bottom row) stimulation with 10 nM CXCL11. Left, staining with anti-LAMP-2; middle, staining with anti-cathepsin-L; right, merged images of LAMP-2 (red), cathepsin-L (green) and overlay (yellow). Original magnification, ×40. Results are representative of three experiments.

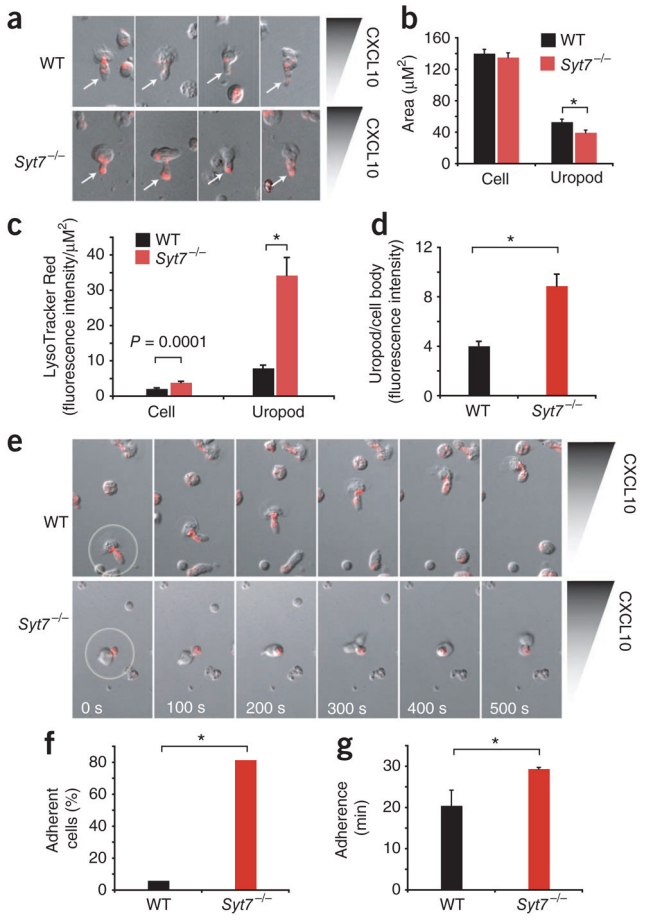

Figure 7.

Localization of LysoTracker Red–stained vesicles during cell migration. (**a**) Confocal microscopy of LysoTracker Red localization during the migration of activated $CD4^+$ lymphocytes from wild-type mice and *Syt7*$^{-/-}$ mice in a gradient (wedge) of CXCL10 (Dunn chemotaxis chamber). Original magnification, ×20. Results are representative of four experiments. (**b**) Cell body and uropod surface area of wild-type and SYT7-deficient activated $CD4^+$ T cells migrating in a CXCL10 gradient. **P* = 0.01 (Student's *t*-test). Data are representative of four experiments (*n* = 20 cells per group; error bars, s.e.m.). (**c**) LysoTracker Red localization in wild-type and *Syt7*$^{-/-}$ activated $CD4^+$ T cells migrating in a CXCL10 gradient. **P* = 0.000001 (Student's *t*-test). Data are representative of four experiments (*n* = 20 cells per group; error bars, s.e.m.). (**d**) LysoTracker Red fluorescence intensity in polarized wild-type and *Syt7*$^{-/-}$ cells (uropod/cell body). **P* = 0.00025 (Student's *t*-test). Data are representative of four experiments (error bars, s.e.m.). (**e**) Laser-scanning confocal microscopy of polarized, activated wild-type and *Syt7*$^{-/-}$ $CD4^+$ lymphocytes (time series). Outlines (far left) indicate initial locations of polarized cells followed over time in the subsequent images. Original magnification, ×20. Results are representative of four experiments. (**f**) Adherence of polarized wild-type cells (*n* = 114) and *Syt7*$^{-/-}$ cells (*n* = 108) over a 30-minute period. **P* = 8.3×10^{-30} (χ^2 test). Data are representative of four experiments (error bars, s.e.m.). (**g**) Duration of the adhesion of polarized adherent wild-type cells (*n* = 6) and S*yt7*$^{-/-}$ cells (*n* = 88). **P* = 0.00000045 (Student's *t*-test). Data are representative of four experiments (error bars, s.e.m.).